Soft Matter

View Online
Dynamic Article Links

Cite this: *Soft Matter*, 2011, **7**, 3268

www.rsc.org/softmatter

COMMUNICATION

Block copolymer self-organization *vs.* interfacial modification in bilayered thin-film laminates

Arif O. Gozen,†[a] Jiajia Zhou,[c] Kristen E. Roskov,[a] An-Chang Shi,[c] Jan Genzer[a] and Richard J. Spontak*[ab]

Received 16th October 2010, Accepted 28th January 2011
DOI: 10.1039/c0sm01169j

Block copolymers remain one of the most extensively studied and utilized classes of macromolecules due to their extraordinary abilities to (i) self-assemble spontaneously into a wide variety of soft nanostructures and (ii) reduce the interfacial tension between, and thus compatibilize, immiscible polymer pairs. In bilayered thin-film laminates of immiscible homopolymers, block copolymers are similarly envisaged to stabilize such laminates. Contrary to intuition, we demonstrate that highly asymmetric block copolymers can conversely destabilize a laminate, as discerned from macroscopic dewetting behavior, due to dynamic competition between copolymer self-organization away from and enrichment at the bilayer interface. The mechanism of this counterintuitive destabilization is interrogated through complementary analysis of laminates containing mixtures of stabilizing/destabilizing diblock copolymers and time-dependent Ginzburg–Landau computer simulations. This combination of experiments and simulations reveals a systematic progression of supramolecular-level events that establish the relative importance of molecular aggregation and lateral interfacial structuring in a highly nonequilibrium environment.

One of the most important technological challenges in the development of inexpensive polymeric materials with tailored properties is compatibilization of two or more immiscible homopolymers.[1] The demand for such polymeric systems continues to grow as the need for lightweight, processable and mechanically robust materials increases in response to efforts aimed at conserving natural resources and reducing energy consumption.[2] Most polymer pairs are inherently immiscible due to unfavorable thermodynamics:[3] the enthalpy of mixing is typically endothermic and the entropy of mixing is often negligibly small. Compatibilization requires a reduction in interfacial tension, which, in turn, is achieved through a variety of interfacial modification strategies.[4] One effective route is reactive blending,[5,6] which relies on the chemical coupling of dissimilar macromolecules at the polymer/polymer interface. The result is the *in situ* development of block (or graft) copolymer molecules, which, when localized at the interface, serve to lower the interfacial tension (thereby reducing the size scale of phase separation), improve fracture toughness[7] and prevent phase coalescence.[8] While this approach is broadly applicable to a wide range of polymers and ensures that copolymer molecules reside at the interface where they are needed, it can suffer from undesirable side reactions, as well as low yields since the reactive macromolecules must meet at the interface for the reaction to proceed.

An alternative to reactive blending relies on the physical addition of a premade block copolymer to an incompatible polymer blend.[9] In this case, the copolymer molecules must be allowed to diffuse to the developing polymer/polymer interface. While this can be largely accomplished through the use of plasticizing agents or high shear fields, a fraction of the copolymer population remains inevitably in one or both of the homopolymer phases. In this case, the copolymer molecules in the bulk seek to reduce unfavorable contacts with the surrounding matrix by self-assembling into nanostructured domains that protect their incompatible elements. Alone, diblock copolymers can organize spontaneously into periodic nanostructures ranging from spheres or cylinders of the minority component (on a body-/face-centered cubic or hexagonal lattice, respectively) in a matrix of the majority component to bicontinuous channels or lamellae.[10] In the presence of a solvent or homopolymer, aperiodic bicontinuous[11,12] and network[13] morphologies may also develop. Because of the propensity for block copolymers to self-organize, melt blending of incompatible homopolymers must be conducted in such fashion to keep the population of copolymer molecules remaining in one or both homopolymers relatively low; otherwise, trapped copolymer molecules form aggregates that resemble micelles, which prevent the interface from attaining its maximum strength and hinder compatibilization.

Similar phenomena likewise occur during the copolymer-induced stabilization of bilayered thin-film laminates composed of two molecularly thin homopolymer films. Such laminates are important to the development of advanced protective coatings,[14] solar cells[15] and waveguide assemblies,[16] in which case a detailed understanding of the molecular-level processes governing stabilization is required. In addition, the planar arrangement of such laminates provides a convenient test platform for the exploration of material and/or design variations in systematic fashion[17] while avoiding changes in interfacial curvature that would occur in bulk systems due to

[a]*Department of Chemical & Biomolecular Engineering, North Carolina State University, Raleigh, NC, 27695, USA*
[b]*Department of Materials Science & Engineering, North Carolina State University, Raleigh, NC, 27695, USA. E-mail: Rich_Spontak@ncsu.edu*
[c]*Department of Physics and Astronomy, McMaster University, Hamilton, Ontario, L8S 4M1, Canada*
† Present address: Center for Research & Technology, Bridgestone Americas, Akron, OH 44317, USA.

compatibilization. Without an added copolymer, a laminate may rupture either in a single layer or in both layers,[18,19] forming circular holes or other complex dewetting patterns,[20,21] when heated above the glass transition temperatures of the two constituent homopolymers. Here, we only consider the cases where (i) the melt viscosity of the substrate layer is much larger (by ~6 to 7 orders of magnitude) than that of the top layer so that the substrate may be considered solid-like relative to the top layer;[22] and (ii) destabilization proceeds by the nucleation and growth of rimmed holes that eventually impinge.[18] In the absence of interfacial slip,[23] the hole diameter (D) varies linearly with time (t), and the hole growth (dewetting) rate (dD/dt) depends on the ratio of the dewetting force to the friction caused by viscous dissipation. The magnitude of dD/dt affords a relative measure of interfacial stability and can, along with the mechanism of dewetting, be controlled by varying material parameters such as the thickness[24] or molecular weight[25] of the top layer (*cf.* Fig. 1), as well as by adding a species that modifies the nature of the interface.[25,26]

We prepared thin-film laminates from two polystyrene (PS) homopolymers with number-average molecular weight ($\bar{M}_n$) values of 30 and 50 kDa (PS30 and PS50, respectively), in conjunction with a poly(methyl methacrylate) (PMMA) homopolymer with $\bar{M}_n$ = 243 kDa (PMMA243), all from Pressure Chemical, Inc. (Pittsburgh, PA). To the PS homopolymers, we added poly(styrene-*b*-methyl methacrylate) (SM) diblock copolymers (Polymer Source, Inc., Dorval, Quebec, Canada) varying in molecular symmetry: S10M50, S50M54 and S50M10, where each numerical designation denotes the block molecular weight (in kDa). In all cases, the polydispersity indices reported by the manufacturers were lower than 1.09. These materials, as well as solvent-grade toluene (Sigma-Aldrich, St Louis, MO), were used as-received. Each PMMA243 substrate measuring 50 ± 2 nm thick from ellipsometry was spun-cast at a speed of 2000 rpm onto a silicon wafer from a 1.35 wt% solution in toluene. Similarly, 1.55 wt% solutions of PS30 and PS50 in toluene were spun-cast at the same speed with and without added copolymers onto glass. Each film measured 60 ± 2 nm thick and was floated off on deionized water and then deposited on a PMMA243 substrate to form a bilayered laminate. All laminates were dried for 24 h at ambient temperature and subsequently heated to 180 °C under nitrogen. Dewetting kinetics were monitored in reflection mode with an Olympus BX60 optical microscope equipped with a Mettler heating stage and a computer-interfaced CCD camera. Transmission electron microscopy (TEM; Hitachi HF2000, 200 kV) was performed on laminates prepared on silica-coated grids and exposed to the vapor of RuO_4(aq), which selectively stains the phenyl rings of styrenic moieties. Atomic force microscopy (AFM; Park Systems XE-100) was conducted in non-contact mode on specimens before and after selective removal of the top PS30 layer in 1-chloropentane.[27]

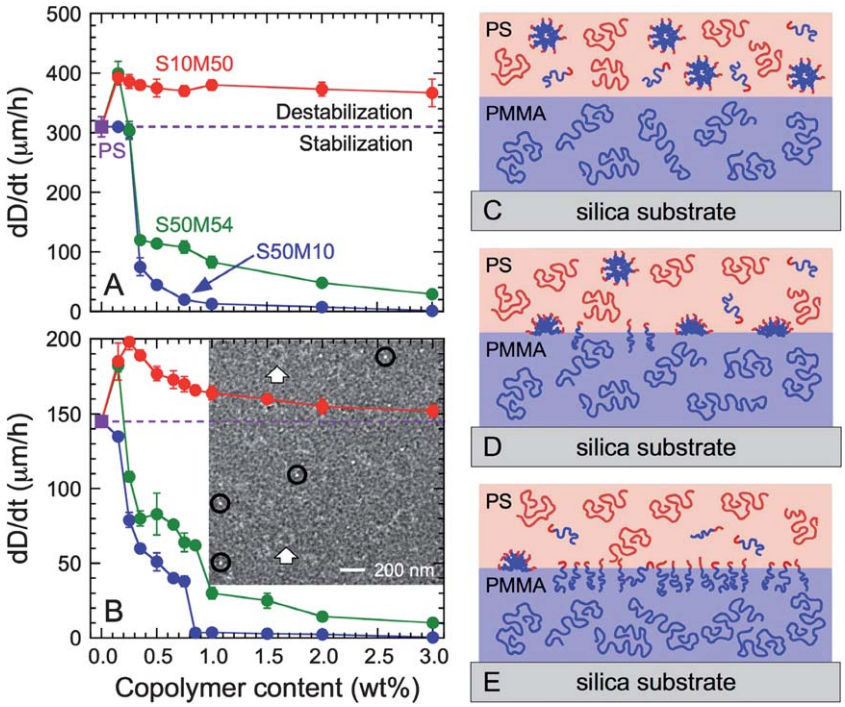

Fig. 1 Dewetting rates (dD/dt) presented as a function of copolymer concentration for laminates with (A) PS30 and (B) PS50 as the top PS layer (labeled in A). Diblock copolymers defined in the text and added to the top layer are likewise color-coded and labeled. Solid lines connect the data, and the dashed line corresponds to the copolymer-free dewetting rate and delineates top-layer stabilization from destabilization. Error bars denote one standard deviation in the data. The TEM image in (B) shows the ill-defined and faint S10M50 nanostructure that develops upon spin-casting a PS50/S10M50 film with 0.75 wt% S10M50 onto glass, followed by floated transfer onto a PMMA243 substrate layer spun-cast on a silica-coated grid. In this image, styrenic units are stained with the vapor of RuO_4(aq) so that unstained methacrylic moieties appear light. Examples of aggregates resembling micelles are circled, whereas more complex shapes are identified by arrowheads. Included are schematic illustrations of the mechanism by which asymmetric S10M50 block copolymers destabilize a bilayered laminate: (C) copolymer molecules self-organize into aggregates (portrayed here), as well as more complex nanostructural elements (*cf.* the inset in B) upon initial casting; (D) copolymer aggregates and chains in the melt diffuse to the polymer/polymer interface where they adsorb and eventually undergo fusion, promoting an increase in interfacial roughness; and (E) additional aggregates form (depending on the available copolymer reservoir) and continue to migrate to and meld with the interface to form copolymer brushes.

Dewetting rates are presented in Fig. 1 as a function of copolymer concentration for laminates composed of PS30 (Fig. 1A) and PS50 (Fig. 1B) top layers on PMMA243. In the absence of copolymer, measured values of dD/dt are 310 ± 17 and 145 ± 4 μm h^{-1}, respectively, confirming that a larger melt viscosity due to increased molecular weight of the top layer reduces dD/dt and thus improves stability.[25] Similarly, these homopolymer dewetting rates can be used to distinguish copolymer-induced stabilization (or destabilization) by discerning whether dD/dt is lower (or higher) than that of the unmodified PS/PMMA243 interface. The dewetting rates with the addition of the asymmetric S50M10 and nearly symmetric S50M54 copolymers (Fig. 1A) verify that both copolymers tend to promote stabilization, with S50M10 being more effective than S50M54. This comparison reveals that, with their long styrenic block and short methacrylic block, S50M10 molecules are less likely to form aggregates in PS30 and therefore diffuse to the interface where they adsorb and physically separate the two homopolymers, thereby reducing interfacial tension. An increase in copolymer concentration further improves the stability of PS30 due to a larger population of copolymer molecules available for interfacial modification. At very low concentrations, however, the S50M54 copolymer is found to induce destabilization due to the presence of the longer, more PS-incompatible methacrylic block. In stark contrast to the general behavior of these copolymers, incorporation of the S10M50 copolymer fully *destabilizes* the PS30 layer over the entire copolymer concentration range examined (with no discernible concentration dependence). The molecular-level mechanism responsible for this unexpected and counterintuitive result is described and discussed below. Similar trends are evident in Fig. 1B for laminates with PS50. Note, however, that in this case the dewetting rates measured for laminates with the S10M50 copolymer decrease with increasing concentration and approach the dewetting rate of the neat PS50.

Comparison of the dewetting rates achieved by adding the S50M10 and S10M50 block copolymers (with identical molecular weights) in Fig. 1 indicates that S50M10 brings about stabilization, whereas S10M50 enhances destabilization. The mechanism by which the S50M10 copolymer improves the compatibility of the immiscible interface has already been discussed, but the behavior of the S10M50 copolymer is more complex, as illustrated in Fig. 1C–E. We hypothesize that the incompatibility between either PS30 or PS50 and the S10M50 molecules, which possess a short styrenic block and a relatively long methacrylic block, is sufficiently high to induce the spontaneous formation of aggregates with methacrylic cores and styrenic shells, as evidenced by the inset of Fig. 1B. These aggregates measure 30 ± 6 nm in diameter and resemble crew-cut micelles[28] (depicted in Fig. 1C). Because they are far from equilibrium, the copolymer molecules are likewise capable of adopting more complex shapes (*e.g.*, vesicles or toroids). As the system evolves, aggregates and individual copolymer molecules migrate (at different rates), and ultimately fuse, to the interface, as portrayed in Fig. 1D. Existence of partially fused, as well as intact, aggregates along the interface causes increases in interfacial roughness and, hence, area, which promote a net increase in free energy and destabilization of the top layer. In this case, the in-plane distribution of copolymer aggregates and molecules is not uniform. Eventual dissolution of aggregates into brush patches (*cf.* Fig. 1E) is expectedly related to the incompatibility between the styrenic matrix and the methacrylic block, which is greater in the PS50 than in the PS30 laminates. This consideration explains why dD/dt is (within experimental uncertainty) independent of copolymer concentration in Fig. 1A, but decreases noticeably with increasing copolymer concentration in Fig. 1B.

Evidence supporting our proposed mechanism can be attained from time-dependent Ginzburg–Landau computer simulations, which were performed with the assumption that the PMMA243 substrate layer can be treated as a PMMA-attractive surface to simplify and accelerate the calculations.[29] A free energy functional proposed[30] previously for AB diblock copolymer/homopolymer blends is incorporated into the Cahn–Hilliard equation to model short-time system dynamics. The spatiotemporal behavior of two asymmetric copolymers configured to emulate the S10M50 and S50M10 molecules, one with 17% A (A17B83) and the other with 83% A (A83B17), is considered in a homopolymer A matrix in terms of (i) an order parameter (ψ) that reflects the local copolymer concentration and (ii) local height variations that provide a measure of roughness and, hence, structuring. The time-dependent variation of ψ in the z direction, where z is normal to the A/B interface (Fig. 2A), shows that the concentrations of both copolymer molecules along the interface ($z = 0$) increase as the system evolves. A striking difference between the two species is that the A17B83 molecules extend from the interface as organized aggregates

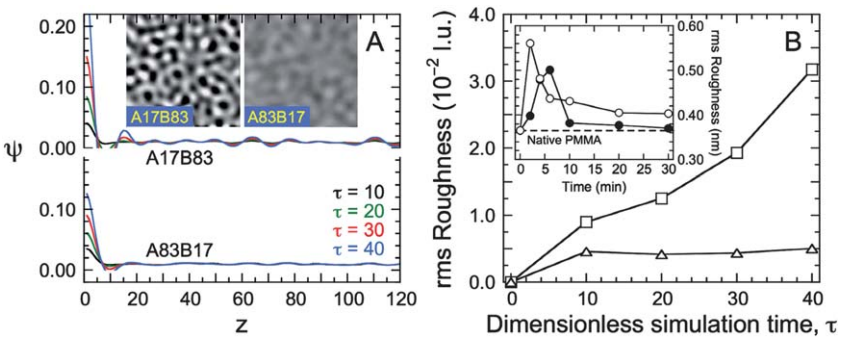

Fig. 2 In (A), the concentration-based order parameter (ψ) presented as a function of distance from the A/B polymer interface (at $z = 0$) at different simulation times (τ, labeled) for A17B83 and A83B17 copolymer molecules (labeled and defined in the text) at a copolymer concentration of 1.0 wt%. A pair of 2D lateral simulation images near the A/B interface at $\tau = 40$ is displayed for both copolymers (labeled) in the inset of (A). Values of the rms roughness (in lattice units, l.u.) extracted from simulation images such as those provided in (A) are provided for the A17B83 (□) and A83B17 (△) copolymers as a function of τ in (B). Included in the inset of (B) are experimental rms roughness values measured by AFM of wet (not dewetted, ○) and dry (dewetted, ●) interfacial regions of a laminate after selective removal of the PS30/S10M50 top layer. The solid lines connect the data.

(evidenced by the fluctuations in ψ), whereas the A83B17 molecules do not. A 2D image of a lateral simulation near the interface for a laminate with A17B83 molecules is provided in the inset of Fig. 2A, and reveals the existence of a complex copolymer morphology loosely reminiscent of the nanostructure in Fig. 1B. In contrast, a corresponding image of the A83B17 molecules displays significantly less lateral structuring. Root-mean squared (rms) roughness values extracted from such 2D simulations are given in Fig. 2B and confirm that the A17B83 molecules are more organized, especially near the interface, than the A83B17 molecules, which is consistent with our proposed mechanism.

Experimental AFM measurements of the interfacial roughness of the PS30/S10M50 laminate after selective removal of the PS30 layer are included for comparison in the inset of Fig. 2B and indicate that, at short times, the roughness discerned from both dry (*i.e.*, dewetted) and wet (*i.e.*, not dewetted) regions on the PMMA243 surface increases as dewetting proceeds, in agreement with simulation results (at different time scales). This increase in roughness is attributed to the attachment and partial fusion of copolymer aggregates along the interface. At longer times, the roughness decreases as copolymer aggregates meld into the PMMA243 substrate. This process is observed and expected to be faster (and more complete) for dry regions exposed to surface tension than for wet regions subjected to lower interfacial tension. Existence of interfacial copolymer structuring due to at least partially fused aggregates is verified by the TEM images presented in Fig. 3A and B for laminates containing 0.15 and 0.75 wt% S10M50, respectively, after 6 min at 180 °C. The dark features on the dry PMMA243 surface distinguish stained styrenic moieties and serve to indicate copolymer-rich interfacial regions. At the low copolymer concentration (Fig. 3A), discrete features possess diameters up to 35 nm, which is consistent with the size of copolymer aggregates expectedly measuring $\sim 4R_g$, where R_g denotes the copolymer gyration radius ($\sim$7 nm). At the higher concentration (Fig. 3B), these features are irregularly shaped and possess a broad size distribution extending up to several hundred nanometres across.

According to experimental observations and simulation results, self-assembly of the S10M50 copolymer molecules occurs rapidly, resulting in the formation of micelle-like aggregates that migrate to and roughen the polymer/polymer interface, consequently destabilizing the top PS layer. In contrast, the mirrored S50M10 copolymer behaves in largely opposite fashion: individual copolymer molecules diffuse to and meld with the interface, where they help stabilize the laminate. To discern the relative importance of these competitive molecular-level mechanisms, we have prepared laminates containing mixtures of these two copolymers and measured the dewetting rates, which are presented in Fig. 4. At 1 and 2 wt% S50M10, the destabilization mechanism dominates. Here, the population of S50M10 molecules is insufficient to modify the polymer/polymer interface, whereas the remaining (and more numerous) S10M50 chains favor self-assembly over interfacial modification. Between 3 and 5 wt% S50M10, however, destabilization at low concentrations precedes stabilization. Stabilization is achieved to different extents by having as little as 10 wt% S50M10 in the S10M50/S50M10 mixture. As seen in Fig. 4, using block copolymer mixtures rather than single copolymers to tune stabilizing/compatibilizing efficacy provides an unexplored route to achieving property control from the ground up. Such control must consider the complex interplay between block copolymer self-assembly and interfacial modification under highly nonequilibrium conditions. Our results using a planar test configuration elucidate

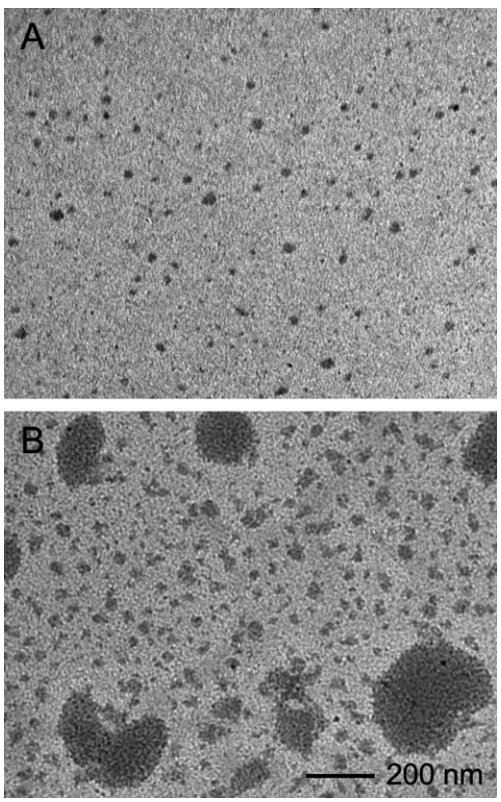

Fig. 3 TEM images acquired from dry regions of annealed laminates with PS50/S10M50 top layers on PMMA243 at two S10M50 concentrations (in wt%): (A) 0.15 and (B) 0.75. Styrene-containing features remaining on the PMMA243 substrate after dewetting appear electron-opaque (dark) due to selective staining.

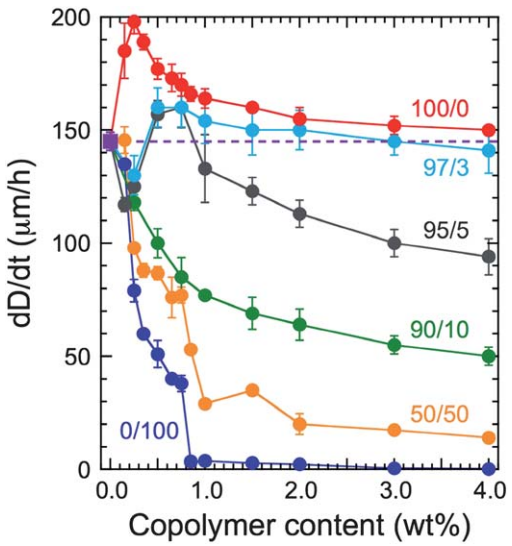

Fig. 4 Dewetting rates presented as a function of total copolymer concentration for PS50/PMMA243 bilayered laminates with and without mixtures of the asymmetric S50M10 and S10M50 block copolymers at different mixture compositions (color-coded, labeled and expressed in w/w S10M50/S50M10). Solid and dashed lines retain their same meanings as in Fig. 1, and the error bars denote one standard deviation in the data.

a molecular-level mechanism responsible for this interplay, which is of critical importance to the contemporary development of tailored polymeric materials.

Acknowledgements

Graduate fellowships for A.O.G. and K.E.R. were provided by Dade-Behring, Inc. and the National Science Foundation, respectively. J.Z. and A.C.S. were supported by the Natural Science and Engineering Council of Canada. The computer simulations were made possible by the facilities of the Shared Hierarchical Academic Research Computing Network (SHARCNET: www.sharcnet.ca) and Compute/Calcul Canada.

References

1 U. Sundararaj and C. W. Macosko, *Macromolecules*, 1995, **28**, 2647–2657.
2 P. Ball, *Made to Measure: New Materials for the 21st Century*, Princeton University Press, New Jersey, 1997.
3 P. J. Flory, *Principles of Polymer Chemistry*, Cornell University Press, New York, 1953.
4 C. E. Koning, M. van Duin, C. Pagnoulle and R. Jérôme, *Prog. Polym. Sci.*, 1998, **23**, 707–757.
5 C. A. Orr, J. J. Cernohous, P. Guegan, A. Hirao, H. K. Jeon and C. W. Macosko, *Polymer*, 2001, **42**, 8171–8178.
6 H. Pernot, M. Baumert, F. Court and L. Leibler, *Nat. Mater.*, 2002, **1**, 54–58.
7 C. Creton, E. J. Kramer, C.-Y. Hui and H. R. Brown, *Macromolecules*, 1992, **25**, 3075–3088.
8 S. Lyu, T. D. Jones, F. S. Bates and C. W. Macosko, *Macromolecules*, 2002, **35**, 7845–7855.
9 A. V. Ruzette and L. Leibler, *Nat. Mater.*, 2005, **4**, 19–31.
10 I. W. Hamley, *The Physics of Block Copolymers*, Oxford Univ. Press, New York, 1998.
11 H. Jinnai, Y. Nishikawa, M. Ito, S. D. Smith, D. A. Agard and R. J. Spontak, *Adv. Mater.*, 2002, **14**, 1615–1618.
12 P. Falus, H. Xiang, M. A. Borthwick, T. P. Russell and S. G. J. Mochrie, *Phys. Rev. Lett.*, 2004, **93**, 145701.
13 S. Jain and F. S. Bates, *Science*, 2003, **300**, 460–464.
14 C. K. Tan and D. J. Blackwood, *Corros. Sci.*, 2003, **45**, 545–557.
15 E. J. W. Crossland, M. Kamperman, M. Nedelcu, C. Ducati, U. Wiesner, D. M. Smilgies, G. E. S. Toombes, M. A. Hillmyer, S. Ludwigs, U. Steiner and H. J. Snaith, *Nano Lett.*, 2009, **9**, 2807–2812.
16 D. H. Kim, K. H. A. Lau, J. W. F. Robertson, O. J. Lee, U. Jeong, J. I. Lee, C. J. Hawker, T. P. Russell, J. K. Kim and W. Knoll, *Adv. Mater.*, 2005, **17**, 2442–2446.
17 S. Zhu, Y. Liu, M. H. Rafailovich, J. Sokolov, D. Gersappe, D. A. Winesett and H. Ade, *Nature*, 1999, **400**, 49–51.
18 G. Reiter, *Phys. Rev. Lett.*, 1992, **68**, 75–78.
19 J. P. de Silva, M. Geoghegan, A. M. Higgins, G. Krausch, M. O. David and G. Reiter, *Phys. Rev. Lett.*, 2007, **98**, 267802.
20 R. Xie, A. Karim, J. F. Douglas, C. C. Han and R. A. Weiss, *Phys. Rev. Lett.*, 1998, **81**, 1251–1254.
21 L. Xue and Y. Han, *Prog. Polym. Sci.*, 2011, **36**, 269–293.
22 F. Brochard-Wyart, P. Martin and C. Redon, *Langmuir*, 1993, **9**, 3682–3690.
23 K. Jacobs, R. Seemann, G. Schatz and S. Herminghaus, *Langmuir*, 1998, **14**, 4961–4963.
24 R. Limary and P. F. Green, *Macromolecules*, 1999, **32**, 8167–8172.
25 B. Wei, J. Genzer and R. J. Spontak, *Langmuir*, 2004, **20**, 8659–8667.
26 B. Wei, P. G. Lam, J. Genzer and R. J. Spontak, *Langmuir*, 2006, **22**, 8642–8645.
27 S. E. Harton, J. Luning, H. Betz and H. Ade, *Macromolecules*, 2006, **39**, 7729–7733.
28 L. F. Zhang and A. Eisenberg, *Science*, 1995, **268**, 1728–1731.
29 G. Brown and A. Chakrabarti, *Phys. Rev. A: At., Mol., Opt. Phys.*, 1992, **46**, 4829–4835.
30 T. Ohta and A. Ito, *Phys. Rev. E: Stat. Phys., Plasmas, Fluids, Relat. Interdiscip. Top.*, 1995, **52**, 5250–5260.

